





Palaeoclimatic distribution models predict Pleistocene refuges for the Neotropical harvestman *Geraecormobius sylvarum* (Arachnida: Opiliones: Gonyleptidae)

Luis E. Acosta & Luis M. Vaschetto

To cite this article: Luis E. Acosta & Luis M. Vaschetto (2017) Palaeoclimatic distribution models predict Pleistocene refuges for the Neotropical harvestman *Geraecormobius sylvarum* (Arachnida: Opiliones: Gonyleptidae), *Journal of Natural History*, 51:1-2, 17-32, DOI: [10.1080/00222933.2016.1245450](https://doi.org/10.1080/00222933.2016.1245450)

To link to this article: <http://dx.doi.org/10.1080/00222933.2016.1245450>

 View supplementary material 

 Published online: 18 Nov 2016.

 Submit your article to this journal 

 Article views: 19

 View related articles 

 View Crossmark data 

Palaeoclimatic distribution models predict Pleistocene refuges for the Neotropical harvestman *Geraecormobius sylvarum* (Arachnida: Opiliones: Gonyleptidae)

Luis E. Acosta ^{a,b} and Luis M. Vaschetto ^{a,b}

^aInstituto de Diversidad y Ecología Animal (IDEA), CONICET-Universidad Nacional de Córdoba, Argentina;

^bCátedra de Diversidad Animal I, Facultad de Ciencias Exactas, Físicas y Naturales, U. N. C., Córdoba, Argentina

ABSTRACT

This paper primarily aims to test a Pleistocene refuge-type scenario, as previously proposed for the gonyleptid *Geraecormobius sylvarum*, a semi-deciduous forests dweller in subtropical Argentina, Brazil and Paraguay. Palaeodistributional models of this species were built using MaxEnt for two Last Glacial Maximum (LGM = 21,000 years ago) simulations – Community Climate System Model (CCSM) and Model for Interdisciplinary Research on Climate (MIROC) – and for 6000 years ago (–6k = HCO, the Holocene climatic optimum). Both LGM models retrieved a fragmented pattern. For CCSM, range was split into multiple, scattered fragments. MIROC resulted in very few patches, with a decided range reduction because of a strong humidity drop. Models for –6k recovered a moderate range expansion. No past connection between the core area and the yungas was predicted. Analysis of variables importance showed that two precipitation predictors (bc18, precipitation warmest quarter; bc14, precipitation driest month) and two temperature predictors (bc7, temperature annual range; bc9, mean temperature driest quarter) scored as the most influencing overall. The Limiting Factor analysis recognized them as limiting too, in different parts of the species range. LGM palaeomodels of *G. sylvarum* are compatible with the refuge hypothesis invoked in previous molecular analyses, to explain the high genetic diversity found in the core area. Additionally, the results reinforced the hypothesis of the recent anthropogenic origin of the yungas disjunct populations.

ARTICLE HISTORY

Received 29 April 2016

Accepted 3 October 2016

Online 18 November 2016


KEYWORDS

Quaternary; refuges; palaeodistributions; Holocene climatic optimum; Last Glacial Maximum; MaxEnt

Introduction

The present study is the sequel to a previous contribution (Acosta 2008), in which the bioclimatic preferences of the subtropical species *Geraecormobius sylvarum* Holmberg, 1887 (Opiliones: Gonyleptidae: Gonyleptinae) were analysed, and a Species Distribution Model was built for the first time in a Neotropical harvestman. In that paper, the species'

CONTACT Luis E. Acosta  luis.acosta@unc.edu.ar  Cátedra de Diversidad Animal I, Facultad de Ciencias Exactas, Físicas y Naturales, U. N. C., Av. Vélez Sarsfield 299, X5000JJC Córdoba, Argentina

 Supplemental data for this article can be accessed [here](#).

© 2016 Informa UK Limited, trading as Taylor & Francis Group

range was modelled using an envelope algorithm (Bioclim), with emphasis on its bioclimatic profile. Further Species Distribution Models were then built for other harvestmen in the region (Acosta and Guerrero 2011; Acosta and Vergara 2013; Acosta 2014; Vergara and Acosta 2015), leading to a better understanding (although still preliminary) of the bioclimatic requirements and range constraints in those species. This type of research represents a valid shortcut to approach a relevant subset of the environmental factors underpinning distributions (Fischer et al. 2001; Peterson 2006), especially considering that ecophysiological surveys on the climatic preferences or tolerance ranges of Neotropical harvestmen are almost completely lacking (Curtis and Machado 2007; Santos 2007). In spite of the limited evidence, most authors consider that harvestmen distributions are in general closely associated to environmental conditions, especially humidity (Ringuelet 1959; Acosta 2002; Curtis and Machado 2007). Therefore, bioclimatic variables are expected (and so far, actually proved) to be well-suited predictors for use in Species Distribution Models in this group (Acosta 2008, 2014; Acosta and Guerrero 2011; Acosta and Vergara 2013).

Geraecormobius sylvorum (Figure 1) has some interesting distributional features. It is a conspicuous representative of the 'Misiones opiliogeographical area' (Acosta 2002, 2008), i.e. the harvestmen assemblage spread over most of the Argentinean Misiones Province, and widely extended into adjacent regions in Paraguay and Brazil. 'Misiones' harvestmen dwell principally in the semi-deciduous forests that characterize two contiguous subtropical ecoregions (as defined by Olson et al. 2001): the Alto Paraná Atlantic Forests and the *Araucaria* moist forests (Figure 2), also known as 'Paraná Forest province' and 'Araucaria Forest province', respectively (Morrone 2014). This harvestmen fauna is herein also referred to as 'Paranense', after the classical 'Paranense Biogeographical



Figure 1. Adult male of *Geraecormobius sylvorum*, from Tucumán Province, Argentina. Photo: Gonzalo D. Rubio.

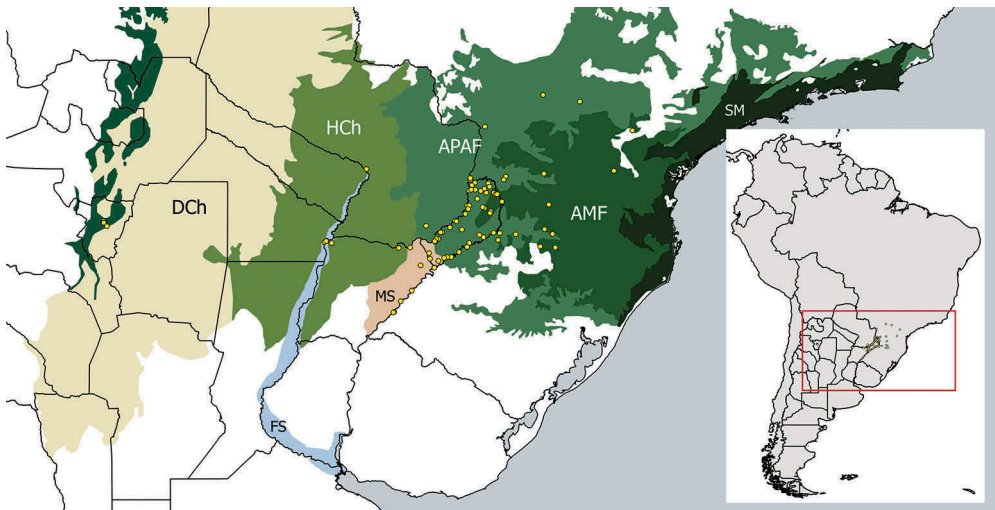


Figure 2. Records of *Geraecormobius sylvarum*, displayed along with the relevant ecoregions in subtropical South America. APAF, Alto Paraná Atlantic forests; AMF, Araucaria moist forests; HCh, Humid Chaco; DCh, Dry Chaco; Y, Southern Andean Yungas; MS, Southern Cone Mesopotamian savanna; FS, Paraná flooded savanna; SM, Serra do Mar coastal forests (nomenclature after Olson et al. 2001).

Region' (Cabrera and Willink 1973), roughly equivalent to the mentioned ecoregions. Models built for *G. sylvarum* using Bioclim demonstrated a remarkable partial match between its predicted range and the Alto Paraná Atlantic Forests, entering marginally into the *Araucaria* moist forests (Acosta 2008). In Argentina, this species also extends southwards and westwards beyond the Alto Paraná Atlantic Forests domains (Figure 2) following gallery forests along two major rivers (Paraná and Uruguay). Presence along the Paraná River is documented up to -56.6833° W (Ituzaingó, near Yacretá Dam), and after a gap (presumably artefactual), it appears again around the confluence with the Paraguay River. On the Uruguay River, the species stretches continuously up to -29.4936° S, near Yapeyú; this part of the range was to a large extent predicted by the Bioclim models (Acosta 2008), before it was confirmed through actual records (Vaschetto et al. 2015). Finally, *G. sylvarum* has a noteworthy range disjunction, depicted by the Bioclim models too, with separate populations in the montane rainforests of Tucumán Province (Southern Andean Yungas ecoregion, northwestern Argentina) (Acosta 2008). Hence, there is a distributional gap of almost 650 km across the sub-heric Dry Chaco ecoregion (Figure 2), an extensive thorny scrubland decidedly unsuitable for most harvestmen species (Acosta 2002, 2008).

A similar disjunction is known for some harvestmen belonging to the adjacent, sub-humid 'Mesopotamian opiliogeographical area' (Acosta 2002), namely *Discocyrtus dilatatus* Sørensen, 1884, *Discocyrtus prospicius* (Holmberg, 1876) and *Gryne oreis* (Sørensen, 1879). In those cases, a historical origin has been suggested for the disjunction, based on Pleistocene climatic cycles (Acosta 1995, 2002; Acosta and Guerrero 2011; Acosta and Vergara 2013). These cycles comprised an alternation of glacial and interglacial periods, in switches between cold and warm climates that were frequently

(though not always) correlated with sub-xeric and humid conditions, respectively (Kröhling and Iriondo 1999; Stevaux 2000; Schreve and Candy 2010). As numerous palynological studies support, those climatic pulses induced vegetational shifts in tropical and subtropical South America, with forests expanding during humid stages, regressing and being replaced by open or more seasonal formations in drier stages (Ledru 1993; Behling 1997, 2002; Ledru et al. 1998, 2009; Behling and Negrelle 2001; Whitney et al. 2014). The invoked scenario was, following Nores (1992), the formation of a forested Mesopotamian–Yungas palaeobridge across the Dry Chaco, during warm-humid periods. Such a suitable corridor might have enabled Mesopotamian harvestmen to expand up to the Yungas, to leave isolated populations as the climate turned drier and humid forests retracted to their current extent. This explanation takes into account the low vagility shown by harvestmen, for which dispersal capabilities (when not mediated by anthropocory) rely almost completely on the continuity of suitable habitats (Acosta 2002, 2008). However, although for Mesopotamian species there is some evidence to support some kind of past connection with the Yungas, this historical scenario does not seem supported for *G. sylvarum*. On the contrary, distribution models based on current climate, along with a preliminary comparison of the genetic structure between Tucumán and the core range, make the disjunct pattern in this species appear more compatible with a recent introduction into northwestern Argentina, rather than with historical events, as discussed by Acosta (2008) and Vaschetto et al. (2015).

The outstanding genetic diversity found in the species core range (Paranense populations) led Vaschetto et al. (2015) to propose a different historical scenario for *G. sylvarum*: its range might have been split into multiple fragments, probably during cool-dry periods in the Pleistocene, a pattern referable to the classical refuge theory (e.g. Haffer 1979, 1982; Prance 1982; Lynch 1988; Bonaccorso et al. 2006). At this point, it emerged as a meaningful goal to test if palaeodistributional predictions of *G. sylvarum* are consistent with the refuge scenario proposed by Vaschetto et al. (2015). Species Distribution Models represent a useful way to estimate past distributions, insofar as palaeoenvironmental information is available (Peterson 2006; Waltari et al. 2007; Kozak et al. 2008). Palaeomodels were preliminarily built for several Mesopotamian species (L. E. Acosta, unpublished), for the Last Glacial Maximum (LGM = 21,000 years ago, or –21k) and the Mid-Holocene *climatic optimum* (HCO = 6000 years ago, or –6k), as representatives of cold-dry conditions and an amelioration stage in the Quaternary, demonstrating species-specific range responses to climate change. Those results encouraged us to reappraise bioclimatic predictions for *G. sylvarum*, so as to project them onto palaeoclimatic conditions. This reassessment was benefited by a larger record set now available, and the use of a modelling method (MaxEnt) that outperforms the previously used Bioclim (Franklin 2009). This paper was aimed to build palaeodistributional models of *G. sylvarum* in contrasting climatic conditions (–21k, –6k), to evaluate the biogeographical scenarios proposed for this species (range splitting in refuge-like fragments; disjunction attributed to anthropic introduction). It was also tested if palaeomodels agree with the general predictions implied in Nores' (1992) postulates (i.e. expansion in –6k, retraction in –21k). To gain a deeper insight of the role of variables in the predictions, different additional analyses were also performed: the relative importance of each predictor was assessed both in general and locally, and their critical response values were determined.

Materials and methods

Data acquisition

The record set (see Supplementary material, Appendix S1) merged localities employed by Acosta (2008), with those recently cited by Vaschetto et al. (2015) and 18 new records introduced in this paper. Localities were either geo-referenced in the field with a Garmin® GPS (own samples), or identified and geo-referenced using printed road maps and Google Earth® (other records). Coordinates of the data set used in Acosta (2008) were thoroughly revised to improve their accuracy. Two (out of three) previously unrecognized records ('Campamento Yacu-Poi, near Puerto Bemberg' and 'Pasarela Río Uruguay': Ringuelet 1959) were now identified and included. In sum, 90 unique point localities (81 effective records, after removal of duplicates from the same grid-cell) were available in this analysis (models in Acosta 2008 were calibrated on 48 records, of which 46 were effective).

Climate layers

Climate surfaces consisted of raster files at a spatial resolution of 2.5 arc-min. Data for current climate were obtained from WorldClim 1.4, a database of average values for 19 bioclimatic (bc) variables encompassing the 1950–2000 period (Hijmans et al. 2005). LGM (–21k) layers were downloaded from the WorldClim website (<http://www.worldclim.org/>), representing two different LGM simulations: CCSM3 (Community Climate System Model; Otto-Bliesner et al. 2006) and MIROC 3.2 (Model for Interdisciplinary Research on Climate; Hasumi and Emori 2004). HCO (–6k) conditions were modelled with the palaeoclimatic layers used by Carnaval and Moritz (2008), based on the ECHAM3 atmospheric general circulation model (DKRZ 1993). The set of 19 bioclimatic variables was reduced to avoid highly correlated predictors (Pearson > 0.80). Pairwise correlation was calculated for temperature and precipitation variables separately (Rissler and Apodaca 2007), on values of 1500 points randomly sampled across the study region. Because knowledge on the ecophysiological meaning of variables is lacking, and to avoid discarding potentially relevant predictors, the choice of one variable in a highly correlated pair was defined by its scoring for relative importance (as explained below) in preliminary models, run with all 19 variables (Acosta 2014). As a result, nine bc variables were selected for use in MaxEnt (Table 1).

Models calibration and accuracy

Current and past distributions were modelled with the maximum-entropy algorithm, MaxEnt (explained in Phillips et al. 2006; Elith et al. 2011), using version 3.3.3k of the free software MaxEnt (Phillips et al. 2011). Preliminary runs were performed to define the best suite of settings for the final analyses, aiming to produce conservative (little permissive) projections for LGM and HCO. Maximum number of background points was set to 20,000, and maximum iterations to 3500. 'Auto' and 'product' features were disabled, selecting all other feature options. The regularization multiplier was left in its default value (=1) and the output of results was set to the logistic option. The analysis

Table 1. Relative importance of the nine bioclimatic (bc) variables used to build the MaxEnt model of *Geraecormobius sylvarum**.

Variable	% bc contribution	Permutation importance	Training gain without	Training gain with only	Overall score
bc18, precipitation of warmest quarter	12.433	44.738	2.827	0.911	55.255
bc7, temperature annual range	14.388	30.256	2.943	1.295	42.997
bc14, precipitation of driest month	37.948	3.488	2.970	1.652	40.118
bc9, mean temperature of driest quarter	16.620	15.652	2.801	1.226	30.696
bc8, mean temperature of wettest quarter	2.560	4.856	2.872	0.523	5.067
bc15, precipitation seasonality	6.662	0.088	2.981	1.286	5.055
bc12, annual precipitation	6.017	0.195	2.982	1.238	4.468
bc2, mean monthly temperature range	2.595	0.440	2.980	0.311	0.367
bc3, isothermality	0.776	0.287	2.974	0.901	-1.010

*Estimators include: (a) percent contribution of each variable to the whole model; (b) permutation importance; (c) jackknife analysis, training gain with each variable set aside at a time; and (d) jackknife, training gain with each variable run in isolation. The four best scores for each estimator are highlighted in grey, the best one in bold. Variables are ordered according to an overall scoring (last column), computing all four estimators (a + b - c + d).

consisted of a 50-replicates run, using the subsample replicate type, with random test percentage set to 10% and 'random seed' selected (73 records to train and eight records to test the model on each replicate). As projections onto past climates may suffer through predicted values being too large, in sites where environmental conditions lie outside the range present in the layers used to build the MaxEnt model (Phillips et al. 2006), 'do clamping' and 'fade by clamping' settings were selected to overcome this problem (in practice, this was only relevant for CCSM projections). To enable simple comparisons and interpretations, suitability was displayed as binary maps for each chronology (current, -6k, CCSM and MIROC; Figure 3). 'Equal training sensitivity and specificity' was the threshold rule applied to sort suitable and not suitable grid-cells, as recommended elsewhere (Liu et al. 2005). Binary predictions summarize all individual 'thresholded' (binary) grids for each chronology; the 50 binary grids were overlaid, retaining as 'suitable' in the final binary map those grid-cells shared by at least 70% of the individual predictions (a little more restrictive cut-off than that used by Acosta 2014). 'Stable' areas, i.e. those considered to have remained suitable for the focal species across the Quaternary, were recognized on the grid-cells shared by binary predictions of all four chronologies (Carnaval and Moritz 2008). Accuracy of the models was measured through the standard area under the curve value (AUC), given in the MaxEnt default results. AUC scores > 0.9 are considered high (Franklin 2009).

Overall importance of variables

The relative importance of each predictor in model building was determined with four different numerical estimators, available in the MaxEnt output (Phillips et al. 2011). These are (a) the percent contribution, (b) the permutation importance, (c) the jackknife analysis, computing training gain with one variable omitted at a time, and (d) the jackknife analysis run with one variable alone. As variables typically rank in a different order for each estimator, final ranking of variables was done in accordance with an 'overall scoring' (a + b - c + d)

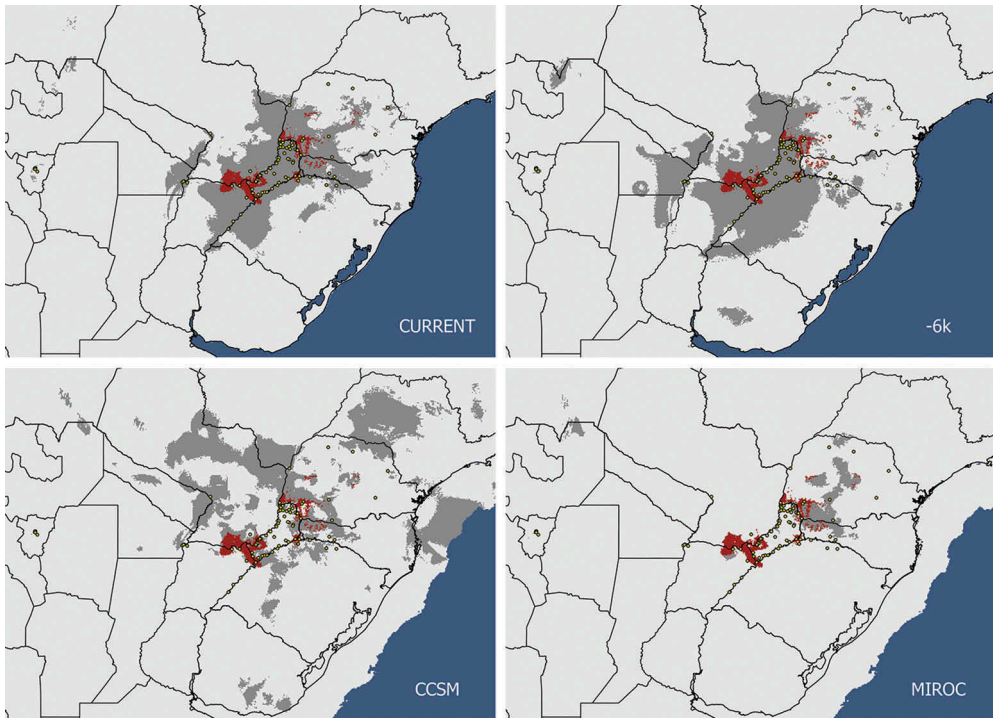


Figure 3. Distribution models of *Geraecormobius sylvarum* for current climate (above left), –6k (above right), –21k CCSM (below left) and –21k MIROC (below right). Maps display the binary prediction (grey), with the stable area highlighted in colour. Small points: presence records. AUC for the 50-replicates run: 0.9839–0.9865; average 0.9854.

(Table 1), as introduced by Acosta and Vergara (2013). As additional information, summary statistics were obtained for all nine variables, to assess basic position and dispersion features of the record set (see Supplementary material, Appendix S2).

Response curves

Marginal response curves yielded by MaxEnt (Phillips et al. 2011), were inspected for the foremost relevant variables, to appraise the critical values at which these predictors contribute the most to the model output. These curves depict changes in the logistic prediction as each environmental variable is varied, while keeping all remaining ones at their average sample value (i.e. curves show the marginal effect of changing a given variable). In Figure 4, marginal curves display the average and \pm SD of the 50 individual curves obtained in the replicated run. Low and high ‘critical values’ in the curves (those delimiting the range in which contribution is effective) were identified where a decided rise or drop of the curve takes place, provided it lies above the 0.5 logistic value and within the empiric values span. The corresponding isotherms and isoyeths (available in the Supplemental Material, Appendix S3) were then visually inspected to track geographical shifts of those lower and higher values for –6k and LGM.

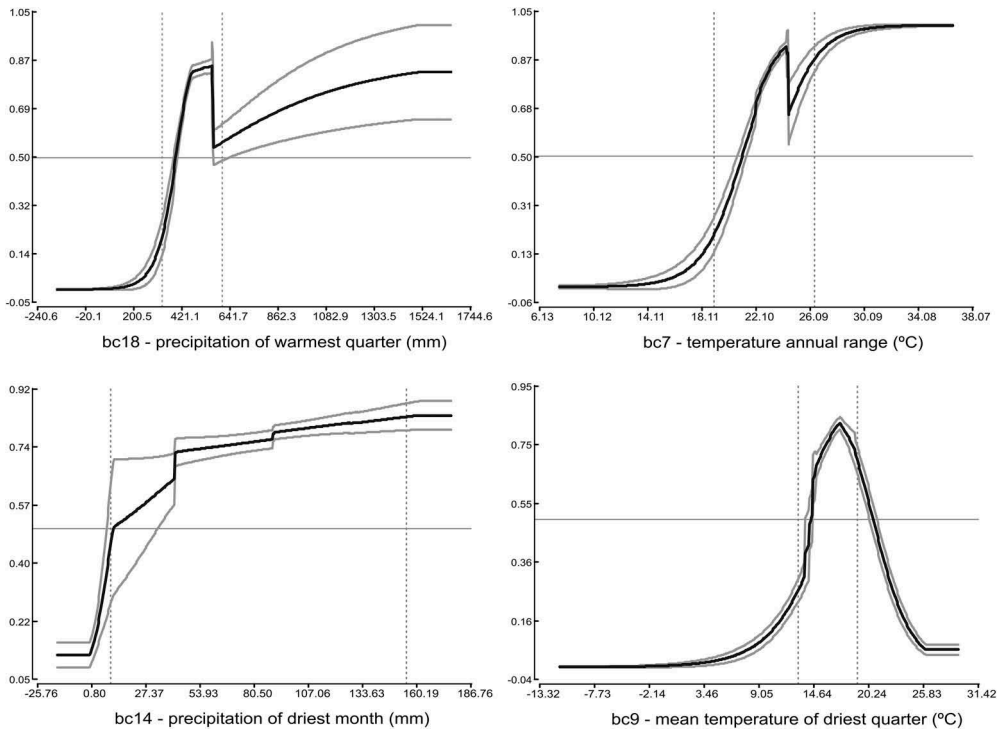


Figure 4. Marginal response curves for the most relevant variables used to model the distribution of *Geraeocormobius sylvarum*. Curves depict average values (black curve) and \pm SD (grey curves) of the 50-replicates run; vertical dotted lines represent the lowest and highest values in the record set, i.e. they delimit the empiric range of the variable. Above: bc18, precipitation of warmest quarter (critical values: 390–560 mm) and bc7, temperature annual range (critical values: 21°C–24.3°C); bottom: bc14, precipitation of driest month (critical value: >42 mm) and bc9, mean temperature of driest quarter (critical values: 14.3°C–18.9°C, peak at 17.3°C). The y-axis displays the logistic probability of presence; horizontal line indicates the 0.50 value.

Local importance of variables

Measures given in Table 1 evaluate the relevance of the variables in the model as a whole. Local differences of this influence were examined using the Limiting Factors analysis, available as a command line extension and performed on the MaxEnt results (Elith et al. 2010). In any grid-cell, the variable whose value influences the model prediction the most is identified as the ‘limiting factor’ at that point. For each variable V_i , its value at a given point P is changed from p_i to the mean value of V_i over the species’ recorded occurrences; the variable for which the change results in the largest model value is the Limiting Factor for the corresponding grid-cell (Elith et al. 2010). The analysis was applied to results of a single run with the full record set and the selected nine variables, for current, –6k, CCSM and MIROC layers, to identify the environmental changes that might explain range shifts.

Results

Present and past range of *Geraecormobius sylvarum*

Current climate

The model looked similar to that previously obtained with Bioclim (Acosta 2008): the suitable area covers all Misiones Province, northeastern Corrientes, the eastern border of Paraguay, as well as several digitations into adjacent Brazil (Figure 3). In the Brazilian State of Paraná, MaxEnt predictions were more restrictive than with Bioclim, leaving outside some northernmost records (Paranavaí, Caviúna). Records from Chaco Province were embraced by a small patch, drawn along the lower Paraguay River but disconnected from the main Misiones sector. Prediction in the Yungas was weak, limited to scattered grid-cells in Tucumán Province (also recovered with Bioclim; Acosta 2008), and other faint patches in Jujuy, northern Salta and southern Bolivia (these sectors were not predicted by Bioclim). Model performances were high, with AUC ranging between 0.9839 and 0.9865 in the 50-replicates run, and an average value of 0.9854.

Palaeodistributional models

Both LGM simulations produced fragmented models (Figure 3). Actually, for CCSM the final suitable area for *G. sylvarum* increased (Table 2), with large and small patches scattered all over the region. Some of these patches reach distant areas not represented in the current model, such as central Paraguay, the State of São Paulo, the continental platform near Santa Catarina (emerged at those times), and as far south as Uruguay. Reduction was extreme in MIROC, representing less than one-quarter of the current area (Table 2). In this model, only two main separate portions remained, one in southern Misiones and northern Corrientes, and an irregular, larger one east of Misiones Province, approximately around the present *Araucaria* ecoregion, with a northwards projection in the centre of the State of Paraná. In contrast, changes in -6k were moderate, with the range in general slightly enhanced (Table 2) and almost no shift (Figure 3). Expansions were verified into western Rio Grande do Sul (Brazil), eastern Paraguay and the still independent Chaco patch; most of the digitations into Santa Catarina and Paraná States suffered a generalized clipping. Some spots in northwestern Argentina persisted in -6k too.

Table 2. Quantification of range changes of *Geraecormobius sylvarum*, as modelled in different chronologies in the Quaternary.*

Current climate Area in km ²	-6k % of current	MIROC % of current	CCSM % of current	Stable area				
				km ²	% of current	% of -6k	% of MIROC	% of CCSM
310,166.8	↑ 120.6	↓ 23.3	↑ 135.6	25,329.5	8	6.8	35	6

*Extension of the predicted area is given in km² for current conditions, and as percent of the current climate distribution for -6k and -21k (MIROC and CCSM). Increase or decrease of range sizes (with respect to current conditions) is indicated with arrows (↑ or ↓). The stable area is the sum of grid-cells shared by models of all chronologies; its extension is estimated in km², stating also the percentage that it represents for current, -6k, MIROC and CCSM predictions.

Stable areas

Suitable grid-cells shared by all chronologies are relatively few, so that the 'stable area' consists of sparse, small isolates (Figure 3), representing altogether < 10% of the prediction for current climate (Table 2); one isolate matches the Misiones-Corrientes patch of the MIROC model, the rest being irregular portions close to the eastern and northern boundaries of Misiones Province. Although all models predicted a patch in northern Salta Province (northwestern Argentina), they do not share any single grid-cell, so that no stable area can be recognized there (Figure 3). In addition to the weak signal obtained in the Yungas, a potential palaeobridge between this ecoregion and the Paranense core area was never recovered.

Importance of variables

Two precipitation and two temperature variables ranked on top for overall relevance: bc18, precipitation of warmest quarter; bc7, temperature annual range; bc14, precipitation of driest month; and bc9, mean temperature of driest quarter (Table 1). These four variables not only represented a 'first line' of importance, but, as stated below, bc18 and bc7 are recognized as limiting factors, with influence in large portions of the species range and beyond (for bc14 and bc9, this influence is geographically more restricted). On a second level, bc8, mean temperature of wettest quarter; bc15, precipitation seasonality; and bc12, annual precipitation ranked with much lower overall scoring (Table 1). Influence of two variables reflecting in some way the thermal stability (bc2, mean monthly temperature range; bc3, isothermality) was extremely weak. Descriptive statistics for all nine variables are given in the Supplementary material (Appendix S2).

Response curves for the relevant variables

Marginal response curves for the four top-ranked predictors are displayed in Figure 4. Response curves of both bc18 and bc7 start with a steady increase up to a peak, followed by a sudden drop. Precipitation of the warmest quarter (bc18) starts critically to add gain to the model at around 390 mm, to decrease abruptly from near 560 mm. In the case of bc7 (temperature annual range), critical values extend from 21°C up to a peak at 24.3°C. The response curve of bc14 is different, with a number of stepwise jumps along a continued increase (Figure 4). This variable starts to be effective at around 42 mm, lacking visible higher restricting values. Hence, it only proved to be limiting at the lower end, which corresponds to records from the Yungas. In that region, decrease of precipitation in the driest month is more accentuated than in the Paranense area. This fact is reflected both in the recognition of localities in northwestern Argentina as outliers and in the rise of bc14 as limiting near that area. Finally, bc9 shows a defined bell-shaped response curve, influencing the model between 14.3°C and the actual highest record at 18.9°C (20.7°C in the curve projection), with a peak around 17.3°C. Isohyets and isotherms delimiting the mentioned optimal ranges for all four variables are depicted in the Supplementary material (Appendix S3; Figures S3.1 to S3.4); there, the most remarkable feature is the strong shift of isolines in MIROC and CCSM, which renders the study area cooler and drier during LGM.

Limiting factors

Current climate

One of the most relevant variables (bc18, precipitation of warmest quarter) proved to be limiting in the southern portion of the core area (Figure 5). This influence extends towards the south and the west, i.e. the direction in which precipitations decrease. In other words, this variable becomes limiting as long as precipitations become scarce (the lowest recorded value for this variable is 331 mm; see Supplementary material, Appendix S2). In contrast, towards northern and eastern regions precipitation does not constitute a serious constraint, and temperature variables become more relevant. There, another top-ranked variable (bc7, temperature annual range) becomes limiting, turning restrictive at lower values (lowest record with 19°C). Other variables proved their limiting character in more reduced areas: bc8, mean temperature of wettest quarter in the central portion of the core area and bc9, mean temperature of driest quarter on eastern, southern and central parts of the range. As stated, precipitation of the driest month (bc14) was critical in an area bordering the Yungas, in northwestern Argentina and southern Bolivia.

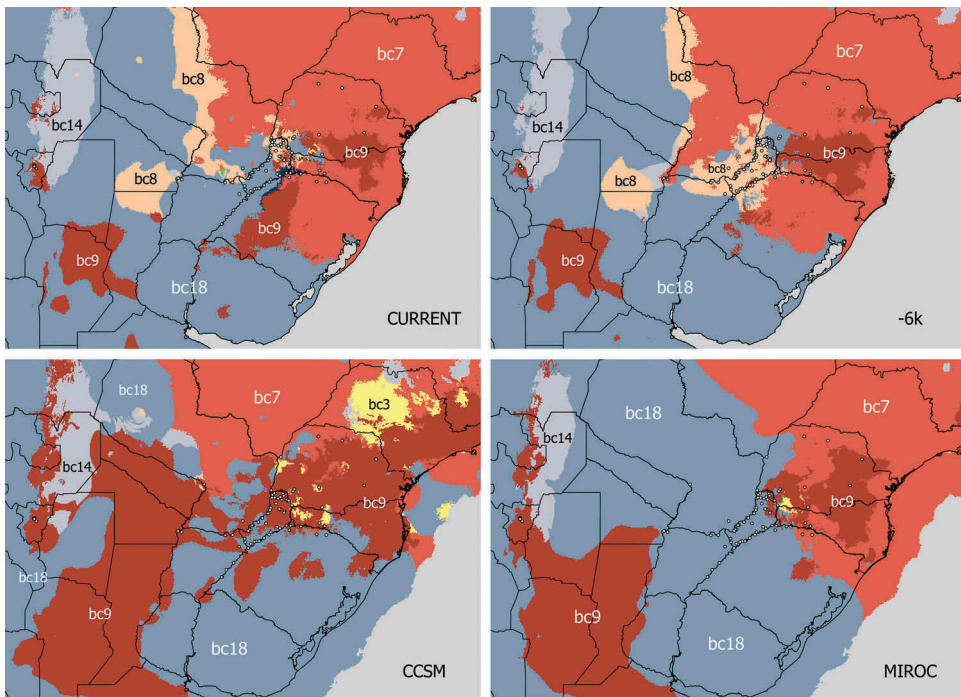


Figure 5. Limiting factor analysis for *Geraecormobius sylvarum*, applied to current climate (above left), –6k (above right), –21k CCSM (below left) and –21k MIROC (below right). Most relevant variables recognized as limiting: bc18, precipitation of warmest quarter; bc7, temperature annual range; bc9, mean temperature of driest quarter; bc8, mean temperature of wettest quarter; bc14, precipitation of driest month and bc3, isothermality. Small points: presence records.

Shifts of limiting variables in -6k, MIROC and CCSM

Limiting factors remain almost the same in -6k (Figure 5), except for bc8 expanding its influence to almost all Misiones Province, and bc9 being enhanced on the eastern side (probably thereby driving the range clipping in that area). Influence of bc9 on the south-eastern margin almost vanishes in -6k, maybe as the region turns cooler, enabling the expansion into Rio Grande do Sul predicted in that period. In LGM's case, regions where bc9 acts as limiting are increased in both simulations. This is especially remarkable in CCSM, in which it displays a patchy appearance around the current core area, recalling the refuge-like predictions of models; also the boundary between bc7 and bc18 displays a 'fragmentary' output. For MIROC, there is a strong northeastward enhancement of the influence of bc18 (revealing a northeastward shift of drought in the warmest quarter), which might be the main factor responsible for the extreme range reduction in that period.

Discussion

The inspection of individual properties of variables is always a valuable tool to start understanding the climatic preferences of a species. Acosta (2008) already described cumulative frequency curves for *G. sylvarum*, useful to overview the frequency distributions of variables and the position of each locality in the bioclimatic range. In this paper, that information is supplemented with an appraisal of the relative contribution of variables, as well as with the marginal response curves, which enabled us to identify the critical values by which each variable adds gain to the model. Although Bioclim models of *G. sylvarum* indicated that temperature variables were collectively more determining than precipitation ones (Acosta 2008), in the present study the top ranking for relevance was shared by two precipitation and two temperature variables. Precipitation of the warmest quarter (bc18) held the highest value for permutation importance and the best overall score, while precipitation of the driest month (bc14) was placed first for percent contribution and in the jackknife test run with that variable alone (so having the most useful information by itself). With respect to temperature variables, bc7, temperature annual range, rated in the second place for the overall score and had all four individual estimators among the four highest values; bc9, mean temperature of driest quarter, was amidst the top four for three estimators, and was ranked the highest for the jackknife test without this variable (i.e. it contains the most information that is not present in the other predictors). In the core area, results of the limiting factor analysis were consistent with the relevance ranking, providing some hints on which predictors might have acted as major drivers of range changes. For current climate, it sounds logical that a temperature variable (bc7, temperature annual range) resulted limiting in the northern portion of the core range, i.e. in a region where rainfall appears 'guaranteed'. In contrast, bc18, a precipitation variable, became limiting at the southern part of the range, that is, where humidity gradually decreases southwards and westwards.

For several variables, especially those reflecting precipitation seasonality, records from the Yungas occupied one end of the distribution (they are outliers in some cases); in fact, climatic conditions of northwestern Argentina represented a marginal portion of the species preferences span. Consequently, as with Bioclim (Acosta 2008), MaxEnt predicted presence in northwestern Argentina very weakly, and this condition was maintained in all

periods, with not a single grid-cell recognized as 'stable'. More importantly, distribution models failed to recover or even insinuate any trace of a Quaternary palaeoconnection. These results weaken evidence for the historical hypothesis, thereby adding some credit to the anthropocoric origin of *G. sylvorum* in the Yungas, as already suggested by current models (Acosta 2008) and the molecular analyses (Vaschetto et al. 2015).

The present research tackled for the first time palaeoclimatic predictions for a Paranense harvestman. As expected, and save a local clipping on the east, $-6k$ predicted a slight *in situ* range expansion. In contrast, the hostile LGM climate affected the species range throughout, be it driven by the marked drop in temperature (CCSM) or in precipitation (MIROC). It is clear that LGM conditions assumed by CCSM and MIROC differ substantially, the latter simulating milder temperatures but more severe drought (cf. Supplementary material, Appendix S3). Those differences advised us that it was better to keep CCSM and MIROC results separate, not trying to merge them in, say, a consensus prediction for $-21k$ (like, for example, averaging them; Bonaccorso et al. 2006). A remarkable prediction of CCSM is the heavy range fragmentation, a pattern consistent with features of molecular diversity shown by this species, in which haplotype and nucleotide diversity was high, and most analysed populations bore unique haplotypes. This resulting concordance from independent sources strengthens the refuge-type scenario suggested by Vaschetto et al. (2015). As seen, counting all suitable patches, CCSM predicts an increased range (Table 2). However, models depict climatic suitability alone (not effective occupation), so these results do not mean that the species was necessarily present in all patches. At least some distant ones (e.g. in Uruguay or in the current continental platform, emerged at those times) look unlikely to have been effectively reached by *G. sylvorum*. Such a scattered predicted area appears to be correlated to the also patchy geographical distribution of some key temperature variables (like bc7 and bc9) and at least one precipitation variable (bc18) in CCSM (see Supplementary material, Appendix S3). In the case of MIROC, results produced a fragmented range too, although reduction is extreme, probably because of the mentioned strong humidity drop. This shrinkage left very small areas recognized as 'stable' across all four chronologies. It remains to be tested whether the exact location of those stable grid-cells represents an accurate prediction or, more likely, these results should be regarded as a coarse initial approach. Indeed, these models were built with data referring to very specific time-slices (LGM, HCO), not to all glacial and interglacial stages that occurred several times along the Quaternary (Schreve and Candy 2010), so any extrapolation should be made cautiously.

The modelling approach demonstrated that range fragmentation in a glacial stage is a plausible scenario for *G. sylvorum*. Palaeodistributional models of further Misiones species should be calibrated, to determine if the refuge hypothesis could be generalized to all Paranense harvestmen.

Geolocation Information

The study area is delimited between $-74.6667^{\circ}W$ / $-35.2083^{\circ}W$, and $-14.1250^{\circ}S$ / $-41.8333^{\circ}S$.

Acknowledgements

For their friendly collaboration in fieldwork, the authors are indebted to Raúl González-Ittig, Julia Vergara, Mónica García and Gonzalo Rubio, the latter also for sharing the photograph of a male

G. sylvorum. Ana Carolina Carnaval and Michelle Koo (Berkeley) kindly enabled us to use their own –6k digital layers, and Jane Elith provided helpful advice to perform the Limiting Factors analysis. LEA is a researcher of the Argentinean Consejo Nacional de Investigaciones Científicas y Técnicas (CONICET).

Disclosure statement

No potential conflict of interest was reported by the authors.

Funding

The present research was supported by CONICET, under grant P.I.P. Res. 918/10; Agencia Nacional de Promoción Científica y Tecnológica, under grant FONCYT-PICT 2007-1296; and SECYT-Universidad Nacional de Córdoba, Argentina, all given to LEA.

ORCID

Luis E. Acosta  <http://orcid.org/0000-0003-3107-1349>

Luis M. Vaschetto  <http://orcid.org/0000-0002-9290-4335>

References

- Acosta LE. 1995. Nuevos hallazgos de *Discocyrtus dilatatus* en Argentina, con notas sobre taxonomía, sinonimia y distribución (Opiliones, Gonyleptidae, Pachylinae). *Rev Arachnol.* 10:207–217.
- Acosta LE. 2002. Patrones zoogeográficos de los opiliones argentinos (Arachnida: Opiliones). *Rev Iber Arachnol.* 6:69–84.
- Acosta LE. 2008. Distribution of *Geraecormobius sylvorum* (Opiliones, Gonyleptidae): range modeling based on bioclimatic variables. *J Arachnol.* 36:574–582.
- Acosta LE. 2014. Bioclimatic profile and potential distribution of the Mesopotamian harvestman *Discocyrtus testudineus* (Holmberg, 1876) (Opiliones, Gonyleptidae). *Zootaxa.* 3821:301–320.
- Acosta LE, Guerrero EL. 2011. Geographical distribution of *Discocyrtus prospicius* (Arachnida: Opiliones: Gonyleptidae): is there a pattern? *Zootaxa.* 3043:1–24.
- Acosta LE, Vergara J. 2013. New records and distribution modeling of *Gryne oreensis* (Sørensen) (Opiliones: Cosmetidae) support the Mesopotamian-Yungas disjunction in subtropical Argentina. *Zootaxa.* 3736:143–158.
- Behling H. 1997. Late Quaternary vegetation, climate and fire history of the *Araucaria* forest and campos region from Serra Campos Gerais, Paraná State (South Brazil). *Rev Palaeobot Palynol.* 97:109–121.
- Behling H. 2002. South and southeast Brazilian grasslands during Late Quaternary times: a synthesis. *Palaeogeogr Palaeoclimatol Palaeoecol.* 177:19–27.
- Behling H, Negrelle RRB. 2001. Tropical rain forest and climate dynamics of the Atlantic lowland, Southern Brazil, during the Late Quaternary. *Quat Res.* 56:383–389.
- Bonaccorso E, Koch I, Peterson AT. 2006. Pleistocene fragmentation of Amazon species' ranges. *Divers Distrib.* 12:157–164.
- Cabrera AL, Willink A. 1973. *Biogeografía de América Latina*. Washington (DC): Organization of American States.
- Carnaval AC, Moritz C. 2008. Historical climate modelling predicts patterns of current biodiversity in the Brazilian Atlantic forest. *J Biogeogr.* 35:1187–1201.
- Curtis DJ, Machado G. 2007. Ecology. In: Pinto-da-Rocha R, Machado G, Giribet G, editors. *Harvestmen: The Biology of Opiliones*. Cambridge (MA): Harvard University Press; p. 280–308.

- Deutsches Klimarechenzentrum [DKRZ]. 1993. The ECHAM3 Atmospheric General Circulation Model. Hamburg: Modellbetreuungsgruppe.
- Elith J, Kearney M, Phillips S. 2010. The art of modelling range-shifting species. *Methods Ecol Evol.* 1:330–342.
- Elith J, Phillips SJ, Hastie T, Dudík M, Chee YE, Yates CJ. 2011. A statistical explanation of MaxEnt for ecologists. *Divers Distrib.* 17:43–57.
- Fischer J, Lindenmayer DB, Nix HA, Stein JL, Stein JA. 2001. Climate and animal distribution: a climatic analysis of the Australian marsupial *Trichosurus caninus*. *J Biogeogr.* 28:293–304.
- Franklin J. 2009. Mapping species distributions: spatial inference and prediction. Cambridge (UK): Cambridge University Press.
- Haffer J. 1979. Quaternary biogeography of tropical lowland South America. In: Duellman WE, editor. The South American herpetofauna: its origin, evolution, and dispersal. Lawrence: The Museum of Natural History, The University of Kansas; p. 107–140.
- Haffer J. 1982. General aspects of the refuge theory. In: Prance GT, editor. Biological diversification in the tropics. New York: Columbia University Press; p. 6–24.
- Hasumi H, Emori S, editors. 2004. K-1 Coupled GCM (MIROC) Tokyo: Center for Climate System Research, University of Tokyo; National Institute for Environmental Studies; Frontier Research Center for Global Change.
- Hijmans RJ, Cameron SE, Parra JL, Jones PG, Jarvis A. 2005. Very high resolution interpolated climate surfaces for global land areas. *Int J Climatol.* 25:1965–1978.
- Holmberg EL. 1876. Arácnidos argentinos. *An. Agric. Rep. Argentina.* 4:1–30.
- Holmberg EL. 1887. Viaje á Misiones. *Bol Acad Nac Ciencias, Córdoba.* 10:5–391.
- Kozak KH, Graham CH, Wiens JJ. 2008. Integrating GIS-based environmental data into evolutionary biology. *Trends Ecol Evol.* 23:141–148.
- Kröhling DM, Iriondo M. 1999. Upper Quaternary palaeoclimates of the Mar Chiquita area, North Pampa, Argentina. *Quat Int.* 57/58:149–163.
- Ledru MP. 1993. Late Quaternary environmental and climatic changes in central Brazil. *Quat Res.* 39:90–98.
- Ledru MP, Mourguiart P, Riccomini C. 2009. Related changes in biodiversity, insolation and climate in the Atlantic rainforest since the last interglacial. *Palaeogeogr Palaeoclimatol Palaeoecol.* 271:140–152.
- Ledru MP, Salgado-Labouriau ML, Lorscheitter ML. 1998. Vegetation dynamics in southern and central Brazil during the last 10,000 yr B.P. *Rev Palaeobot Palynol.* 99:131–142.
- Liu C, Berry PM, Dawson TP, Pearson RG. 2005. Selecting thresholds of occurrence in the prediction of species distributions. *Ecography.* 28:385–393.
- Lynch JD. 1988. Refugia. In: Myers AA, Giller PS, editors. Analytical biogeography: an integrated approach to the study of animal and plant distributions. London: Chapman & Hall; p. 311–342.
- Morrone JJ. 2014. Biogeographical regionalisation of the Neotropical region. *Zootaxa.* 3782:1–110.
- Nores M. 1992. Bird speciation in subtropical South America in relation to forest expansion and retraction. *Auk.* 109:346–357.
- Olson DM, Dinerstein E, Wikramanayake ED, Burgess ND, Powell GVN, Underwood EC, D'Amico JA, Strand HE, Morrison JC, Loucks CJ, et al. 2001. Terrestrial ecoregions of the world: a new map of life on Earth. *BioScience.* 51:933–938.
- Otto-Bliesner BL, Brady EC, Clauzet G, Tomas R, Levis S, Kothavala Z. 2006. Last Glacial Maximum and Holocene climate in CCSM3. *J Clim.* 19:2526–2544.
- Peterson AT. 2006. Uses and requirements of ecological niche models and related distributional models. *Biodivers Inform.* 3:59–72.
- Phillips SJ, Anderson RP, Schapire RE. 2006. Maximum entropy modeling of species geographic distributions. *Ecol Modell.* 190:231–259.
- Phillips SJ, Dudík M, Schapire R. 2011. Maximum Entropy Modeling of Species Geographic Distributions (MaxEnt). Version 3.3.3k. Princeton: Princeton University. Available from: <http://www.cs.princeton.edu/~schapire/maxent/>
- Prance GT. 1982. Forest refuges: evidence from woody Angiosperms. In: Prance GT, editor. Biological diversification in the tropics. New York: Columbia University Press; p. 137–158.

- Ringuelet RA. 1959. Los arácnidos argentinos del orden Opiliones. Rev Mus Arg Cs Nat. 5:127–439. Plates I–XX.
- Rissler LJ, Apodaca JJ. 2007. Adding more ecology into species delimitation: ecological niche models and phylogeography help define cryptic species in the black salamander (*Aneides flavipunctatus*). Syst Biol. 56:924–942.
- Santos FH. 2007. Ecophysiology. In: Pinto-da-Rocha R, Machado G, Giribet G, editors. Harvestmen: The Biology of Opiliones. Cambridge (MA): Harvard University Press; p. 473–488.
- Schreve D, Candy I. 2010. Interglacial climates: advances in our understanding of warm climate episodes. Prog Phys Geogr. 34:845–856.
- Sørensen W. 1884. Opiliones Laniatores (Gonyleptides W.S. olim) Musei Hauniensis. Naturh Tidsskr, Ser. 3. 14:555–646.
- Sørensen W. 1879. Om bygningen af Gonyleptiderne, en Type af Arachnidernes Classe. Naturh Tidsskr, Ser. 3. 12:97–222, Plates I–II.
- Stevaux JC. 2000. Climatic events during the Late Pleistocene and Holocene in the Upper Parana River: correlation with NE Argentina and South-Central Brazil. Quat Int. 72:73–85.
- Vaschetto LM, González-Iltig R, Vergara J, Acosta LE. 2015. High genetic diversity in the harvestman *Geraecormobius sylvarum* (Arachnida, Opiliones, Gonyleptidae) from subtropical forests in north-eastern Argentina revealed by mitochondrial DNA sequences. J Zoolog Syst Evol Res. 53:211–218.
- Vergara J, Acosta LE. 2015. More on the Mesopotamian-Yungas disjunction in subtropical and temperate Argentina: bioclimatic distribution models of the harvestman *Discocyrtus dilatatus* (Opiliones: Gonyleptidae). Zoologia (Curitiba). 32:445–456.
- Waltari E, Hijmans RJ, Peterson AT, Nyári AS, Perkins SL, Guralnick RP. 2007. Locating Pleistocene refugia: comparing phylogeographic and ecological niche model predictions. PLoS ONE. 2:e563.
- Whitney BS, Mayle FE, Burn MJ, Guillén R, Chavez E, Pennington RT. 2014. Sensitivity of Bolivian seasonally-dry tropical forest to precipitation and temperature changes over glacial–interglacial timescales. Veg Hist Archaeobot. 23:1–14.